Special Issue on Multi-Carrier Spread-Spectrum

A new OFDM-CDMA Uplink Concept with M-ary Orthogonal Modulation

ARMIN DEKORSY AND KARL-DIRK KAMMEYER
University of Bremen, FB-1, Department of Telecommunications
P.O. Box 33 04 40, D-28334 Bremen, Germany,
{*dekorsy,kammeyer*}*@comm.uni-bremen.de*

July 19, 1999

Abstract. This paper proposes the application of M-ary orthogonal Walsh modulation for an OFDM-CDMA uplink transmission. Beside the examination of general system properties, it is shown that decision-directed phase estimation represents a channel estimation concept suitable for the new system. The Walsh modulation can also be interpreted as a linear block code with low decoding complexity, and the paper concerns the serial concatenation of convolutional codes (CC) with Walsh modulation. New aspects arise since the CC mainly operates in time domain, and the Walsh modulation is merely arranged in frequency domain. In this context, we derive the bit specific reliability information for maximum likelihood (ML) soft decoding of the CC and discuss the trade-off between coding and spreading in case of sufficient and non-sufficient frequency interleaving. Throughout the discussions, the results are always compared with BPSK modulation performance, and it can clearly be demonstrated that M-ary Walsh modulation significantly outperforms BPSK modulation in all aspects considered in this work.
Although the specific simulations are related to the European Hiperlan/2 standardization, the results are valid in general.

1 INTRODUCTION

For mobile communication systems with high data rates, Orthogonal Frequency Division Multiplexing (OFDM) has received a lot of attention in the recent few years. Despite of some advantages like simple one-tap equalization, OFDM has to be combined with diversity techniques to exploit the multipath fading channel [1, 2, 3, 4, 5]. In this paper, we consider the scheme where each information symbol is spread in frequency direction by simple replication of the symbol into parallel subcarriers and additional multiplication of each subcarrier with one code-chip being constant in time. This concept was first introduced as OFDM-code-division multiple access (OFDM-CDMA) or also as multi-carrier (MC-)CDMA by [1, 6] and is also called MC-spread-spectrum (MC-SS).
Most publications dealing with OFDM-CDMA have been focused on *standard modulation schemes* such as M-PSK. Detection methods have been proposed [4, 7, 8, 9], novel channel estimation techniques have been analyzed mainly based on using redundancy like pilot-symbols [10, 11], and several maximum likelihood (ML) decoding strategies have been examined [12, 13, 14].

With simple replication of the information into several diversity branches, M-PSK modulation concepts *slightly profit by CDMA flexibility*, e.g. from the already given frequency resolution of the total bandwidth in case of OFDM-CDMA. Thus, instead of M-PSK modulation, CDMA techniques generally allows to apply *M-ary orthogonal modulation* which has favorable signal properties [15, 16]. A well-known scheme is the QUALCOMM system (IS-95) that is based on single carrier direct sequence CDMA (DS-CDMA)[17, 16].
In order to benefit from OFDM properties (e.g. one-tap equalizer), we propose the application of *M-ary Walsh modulation* as a specific form of M-ary orthogonal modulation for OFDM-CDMA transmission [18]. Since an OFDM-CDMA scheme offers a frequency resolution by dividing the available bandwidth into a finite number of subchannels, the idea behind the application of M-ary Walsh modulation is to increase this resolution in order to better distinguish transmitted symbols. Thus, we optimize the inner spreading of an OFDM-CDMA system [19]. This optimization is carried out by spreading in two successive steps with the constraint of a constant overall bandwidth: (i) spreading by the Walsh modulation itself and (ii) additional simple replication of the information to be transmitted into parallel subcarriers to perform CDMA technique.

The main objective of this paper is to examine the application of M-ary Walsh modulation for OFDM-CDMA systems operating in frequency-selective, slowly Rayleigh fading channels in the uplink. Due to the asynchronous received user signals, the proposed OFDM-CDMA uplink transmission system uses *non-optimized sequences* for user separation. This suggestion avoids high synchronization complexity with the drawback of high multiple access interference (MAI).
We first describe the inclusion of the M-ary Walsh modulation into an OFDM-CDMA system and derive general system properties like spectral efficiency and user-interference. Furthermore, we study the influence of different well-known equalization techniques [12] on the inherent orthogonality of the proposed modulation assuming perfect channel estimation.
Since this orthogonality is extremely sensitive to phase rotation, the equalization scheme used should preferably correct these phase deviations. For channel estimation, the application of decision-directed (DD) phase estimation based on the DD loop technique [15] is suggested. With this method, *no additional information*, i.e. training data, is required yielding a better spectral efficiency in comparison with pilot-symbol-aided channel estimation concepts [10].
M-ary Walsh modulation can also be viewed as a *systematic linear block code* with code rate $\log_2(M)/M$. This interpretation opens a completely new point of view especially with additional convolutional coding (CC) [20]. In this sense, the proposed system represents *a serial concatenated coding scheme operating in time as well as in frequency domain*: the CC as an outer code which is mainly arranged in time direction, and the Walsh modulation as an inner block code merely working in frequency direction. Consequently, the proposed system exploits diversity in time as well as frequency domain and describes a powerful coding scheme which is required in CDMA uplink transmission with inherent high MAI. In the context of channel coding, we will derive the *bit specific reliability information* to perform ML soft decoding of the outer CC. For an optimized design, the trade-off between the CC, M-ary orthogonal modulation and simple spreading in case of sufficient and insufficient frequency interleaving will be discussed by Monte-Carlo simulations. The results are compared with antipodal transmission and are based on the European HIPERLAN/2-standardization, but they are generally valid. Throughout the paper, we assume perfect channel synchronization of the user concerned.

This paper is organized as follows: In Section 2, we present the OFDM-CDMA transmitter with M-ary Walsh modulation, and the most important properties of the modulation concept are briefly introduced. In Section 3, coherent reception of M-ary orthogonal modulated signals is examined, general system properties are derived and different equalization techniques are analyzed. Decision-directed phase estimation is investigated in Section 4. Section 5 describes aspects of serial concatenated coding, and Section 6 concludes the paper.

2 OFDM-CDMA Transmission with M-ary Orthogonal Modulation

2.1 Transmitter

An OFDM-CDMA transmitter with M-ary Walsh modulation is illustrated in Fig. 1. For simplicity, one of J active users is shown and corresponding subscripts are omitted. The data bits, $b \in \{0, 1\}$ each of duration T_b, are

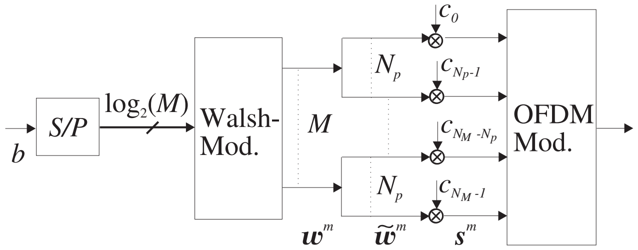

Figure 1: OFDM-CDMA transmitter with Walsh modulation

serial-to-parallel converted to groups of $\log_2(M)$ data bits each. The M-ary Walsh modulation maps the $\log_2(M)$ data bits to the corresponding Walsh symbol (vector) $\boldsymbol{w}^m = [w_0^m, w_1^m, \ldots, w_{M-1}^m]^T$, $m \in \{0, \ldots, M-1\}$ including M Walsh chips $w_\mu^m \in \{\pm 1\}$, $\mu = 0, \ldots, M-1$. Each of the M parallel Walsh chips has a symbol duration of $T = \log_2(M)\, T_b$; thus, with this modulation, frequency spreading of value $M/\log_2(M)$ is achieved. In contrast to the application of the Walsh modulation in DS-CDMA based systems [17], be aware that for OFDM-CDMA each Walsh symbol is arranged in frequency direction.
The set of M Walsh symbols represents an orthogonal basis which can be evaluated recursively by using

$$\boldsymbol{W}_{2M} = \begin{pmatrix} \boldsymbol{W}_M & \boldsymbol{W}_M \\ \boldsymbol{W}_M & -\boldsymbol{W}_M \end{pmatrix}, \quad \boldsymbol{W}_1 = (1), \qquad (1)$$

where $\boldsymbol{W}_M$ is the $M \times M$ Hadamard-Matrix [15, 16]. An important parameter to characterize modulation concepts is the Euclidian distance. For an M-ary Walsh modulation, the Euclidian distance is identical for all possible pairs of symbols and equals

$$\varepsilon = \sum_{\mu=0}^{M-1} |w_\mu^m - w_\mu^n|^2 = 2M \quad \forall \quad m \neq n, \qquad (2)$$

i.e. the Euclidian distance raises with M. Furthermore, it is easily verified that the symbol energy is the same for all symbols. Hence, the latter property together with the raising Euclidian distance leads to a favorable signal space and plainly points out the idea to apply this modulation scheme as an optimization of the inner spreading for a CDMA system.
In order to obtain the symbols to be transmitted, the Walsh

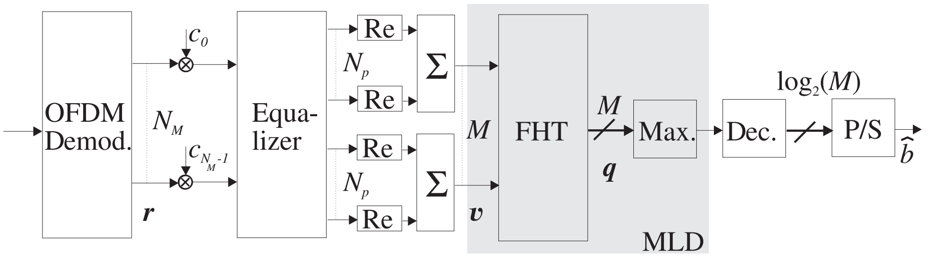

Figure 2: Ideal coherent OFDM-CDMA receiver with MLD of Walsh symbols

chips are replicated into N_p parallel copies. Each branch of the parallel stream is multiplied with one chip of the user specific Pseudo-Noise (PN)-code $c_i \in \{\pm 1/\sqrt{N_M}\}$, $i = 0, \ldots, N_M - 1$, and $N_M = MN_p$ indicates the number of subcarriers. With the application of PN-sequences, synchronization of the signals received from different users is not required, hence, high synchronization complexity can be avoided. For the j-th user, we obtain the transmission vector

$$\boldsymbol{s}^{m,j} = [s_0^{m,j}, \ldots, s_{N_M-1}^{m,j}]^T, \quad s_i^{m,j} = \tilde{w}_i^{m,j} \cdot c_i^j \tag{3}$$

with $\tilde{w}_i^{m,j} = w_\mu^{m,j}, \ \forall \ \mu = \lfloor i/N_p \rfloor, m, j$. OFDM modulation includes the IDFT and inserts the guard interval between adjacent OFDM symbols.

2.2 Channel

In order to prevent intersymbol interference (ISI) and adjacent channel interference (ACI), the guard time T_g is chosen such that $T_g \geq \tau_{max}$, where τ_{max} is the maximum delay of the channel. Due to the insertion of the guard interval, the channel can be described for each user by an $N_M \times N_M$ diagonal matrix $\boldsymbol{H}^j$ with elements H_i^j, with $j = 0, \ldots, J-1$ and $i = 0, \ldots, N_M - 1$ [7]. The transfer coefficients H_i^j are assumed to be zero mean Gaussian distributed random variables according to the Gaussian Wide Sense Stationary Uncorrelated Scattering (GWSSUS) channel model [21].

For comparison of the different systems described in this paper, the chosen channel parameters are all related to the European HIPERLAN/2 standardization for indoor transmission. In particular, the bandwidth is set to $B = 25$ MHz in the 5.2 GHz range. A velocity of $v_0 = 0.5$ m/s results in a very low maximum Doppler frequency $f_{d,max}$ of about 9 Hz. In some cases specially marked, we also uses a velocity of $v_0 = 3$ m/s or $f_{d,max} \approx 54$ Hz, respectively. Thus, the requirement of a time invariant channel within an OFDM symbol duration is fulfilled, even for high M-ary orthogonal modulation leading to long symbol durations T. Moreover, an exponential delay power spectrum with a maximum delay of $\tau_{max} \approx 350$ ns and a coherence bandwidth of the channel of about 2.8 MHz is assumed. Hence, for the employed slowly fading channel, the fading on different subcarriers is statistically dependent (depending on the frequency distance between the considered subcarriers).

3 Coherent OFDM-CDMA Reception with M-ary Walsh Demodulation

3.1 Receiver

In Fig. 2, we present the OFDM-CDMA receiver with M-ary Walsh demodulation assuming perfectly known channel coefficients, called ideal coherent receiver. For J active users and with channel matrix $\boldsymbol{H}^j$ (2.2), the signal after OFDM demodulation can be written as a sum of vectors $\boldsymbol{r}^{m,j}$

$$\boldsymbol{r} = \sum_{j=0}^{J-1} \boldsymbol{r}^{m,j} + \boldsymbol{n} = \sum_{j=0}^{J-1} \boldsymbol{H}^j \boldsymbol{s}^{m,j} + \boldsymbol{n}. \tag{4}$$

The elements of the received vector $\boldsymbol{r}^{m,j}$ can be expressed by $r_i^{m,j} = s_i^{m,j} \cdot H_i^j, \quad i = 0, \ldots, N_M - 1$ and $m \in \{0, \ldots, M-1\}$, where $s_i^{m,j}$ is given by (3). The vector $\boldsymbol{n}$ represents Additive White Gaussian Noise (AWGN). After multiplication with the user specific PN-sequence and equalization, the first part of despreading is obtained by correlation of N_p subcarriers. In the following, reception for the user $j = 0$ is assumed with loss of generality. The components of $\boldsymbol{v}$ are given by

$$v_\mu = \sum_{i=\mu N_p}^{(\mu+1)N_p-1} \mathrm{Re} \left\{ c_i^0 E_i^0 r_i^{m,0} + \sum_{j=1}^{J-1} c_i^0 E_i^0 r_i^{m,j} + c_i^0 E_i^0 n_i \right\}, \tag{5}$$

where E_i^0 indicates the equalization coefficient of the i-th subcarrier, and $\mu, m \in \{0, \ldots, M-1\}$. For our purpose, we take into account the well-known equalization techniques [4, 12]

Orthogonal Restoring Combining (ORC): $\quad E_i^0 = 1/H_i^0$

Equal Gain Combining (EGC): $\quad E_i^0 = e^{-j\,arg(H_i^0)}$

Maximum Ratio Combining (MRC): $\quad E_i^0 = (H_i^0)^*$

$$\text{Soft-ORC}_\gamma : E_i^0 = \left\{ \begin{array}{cl} 1/H_i^0 & \text{for}\,|H_i^0| > \gamma \\ \frac{1}{\gamma} \cdot e^{-j\,arg(H_i^0)} & \text{for}\,|H_i^0| \leq \gamma \end{array} \right. \tag{6}$$

In order to enable maximum likelihood detection (MLD), the vector $\boldsymbol{v}$ is correlated with all Walsh symbols $\boldsymbol{w}^m$, $m \in \{0, \ldots, M-1\}$. The MLD can be realized by the Discrete Hadamard Transform (DHT) ([1]) [16], using the Hadamard matrix (1) according to

$$\boldsymbol{q} = \boldsymbol{W}_M \cdot \boldsymbol{v}. \tag{7}$$

Vector $\boldsymbol{q}$ includes M decision variables, where the choice of the maximum value results in symbol decision. Decoding of the decided symbol to $\log_2(M)$ data bits and parallel/serial conversion finally leads to the estimated data stream with bits $\hat{b}$.

3.2 COMPARISONS OF SYSTEM CONFIGURATIONS

3.2.1 General System Properties

For an OFDM-CDMA system with M-ary orthogonal modulated signals, the data rate is given by

$$R = \frac{\log_2(M)}{M N_p} \underbrace{(1 - \frac{T_g}{T})}_{\alpha} B, \tag{8}$$

where α can be interpreted as the spectral efficiency with respect to the guard interval. For our system comparisons, we assume that

$$\frac{\log_2(M)}{M N_p} \stackrel{!}{=} const. \quad \forall M. \tag{9}$$

Since the system is based on binary modulation, the number of subcarriers is determined by

$$N_M = N_2 \cdot \log_2(M) = M \cdot N_p, \tag{10}$$

where N_2 is the number of subcarriers used for binary Walsh or BPSK modulation, respectively. A large number of users can be taken into account as AWGN (central limit theorem). This results in the user interference $\beta_{int} \approx (J-1)/N_M$ in case of PN-codes. Consequently, we obtain less MAI by raising M due to a higher number of subcarriers (10).
Furthermore, it should be mentioned that using a guard interval results in mismatching

$$\frac{S}{N} = \frac{E_s}{N_0} \underbrace{(1 - \frac{T_g}{T})}_{\alpha}, \tag{11}$$

where E_s is the information symbol energy in the bandpass, $N_0/2$ indicates the two-sided noise spectral density, and S/N is the signal-to-noise (SNR) ratio used for MLD. Since T_g remains the same for all considered values of M, the spectral efficiency α is increased by raising M due to an increasing T. This finally results in less mismatching (11), and with (9) and (8) in a higher data rate. In order to make these relationships more plain, Table 1 shows the amount of mismatching $\Delta E_s/N_0$ in dB and the normalized spectral efficiency α/α_{ideal}, where α_{ideal} denotes the spectral efficiency for a guard time equal zero. These and all the further results of this paper are based on a binary modulation design with $T_g/T = 0.2$. Table 1 clearly demonstrates that it is possible to reach a gain of 0.8 dB in E_s/N_0 by raising M from 2 to 32, and for $M = 32$, we merely loose 5% spectral efficiency.

Table 1: Examples of mismatching and spectral efficiency for M-ary Walsh modulation

M	$\Delta E_s/N_0$ in dB	α/α_{ideal}
2	1	80%
8	0.3	92%
32	0.2	95%

3.2.2 Indoor Channel

OFDM-CDMA belongs to the class of transmission systems, where we have multiple replicas of the same information bearing signal, received over different diversity branches. For these systems, MRC (6) is the optimum diversity combining technique in the ML sense, i.e. it maximizes the SNR assuming AWGN [15, 22].
On the other hand, MRC is conditionally applicable for systems with inherent orthogonality. A specific example is an OFDM-CDMA system for downlink transmission using orthogonal codes to separate the users [4, 11, 12]. Previous work on this system indicates significant degradations of the bit-error-rate (BER) in comparison with combining techniques like EGC or SORC$_\gamma$ [4, 12]. Furthermore, the most promising equalization methods are Wiener-Filtering addressing the issues of the orthogonality to separate the users of an OFDM-CDMA downlink transmission, which is optimum in the mean-square error (MSE) sense [9], or maximum likelihood sequence estimation (MLSE) [12], but both with the drawback of higher complexity effort.

Our proposed system also uses orthogonality, but, instead of separating the users, we separate the information of one user. In particular, we consider an uplink scenario including the application of PN-codes for user separation, and for a large number of users, the user interference can be regarded as AWGN. In order to accomplish demodulation, MLD of the Walsh symbols is employed (Fig. 2). Thus, MRC is expected to be the optimum diversity combining method in the ML sense, although it leads to a high deterioration of Walsh modulation orthogonality.
In order to answer the question for the most applicable diversity combining method, we focus on the standard equalization schemes described in section 3.1 ([2]). Afterwards,

[1]For practical issues, the DHT can be realized by the Fast Hadamard Transform (FHT) [22].

[2]Optimization in the MMSE sense has not yet been studied and could be considered in future work.

the general bit-error performance of the Walsh modulation is investigated and compared with BPSK modulation. All given results refer to the channel described in section 2.2 and have been achieved by Monte-Carlo simulations.

Fig. 3 shows the BER for 32-ary Walsh modulation versus $\bar{E}_b/N_0$ for the equalization methods ORC, SORC$_\gamma$, EGC and MRC (6). The system design refers to binary modulation with $N_2 = 64$ and $T_g/T = 0.2$, and $J = 8$ active users are taken into account. First of all, it turns out

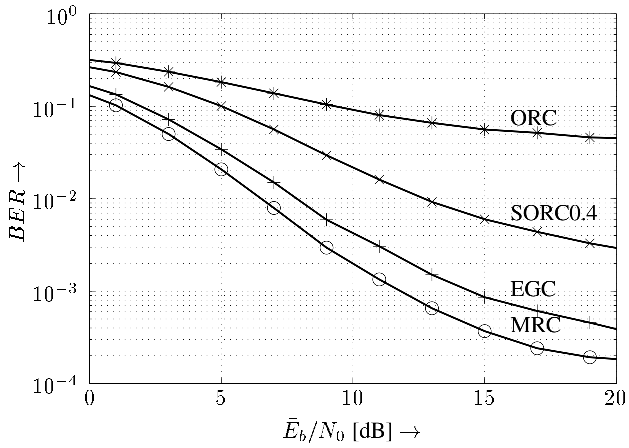

Figure 3: Comparison of diversity combining methods for 32-ary Walsh modulation, $J = 8$ active users, and $N_2 = 64$ subcarriers

that ORC performs worst due to the well-known noise amplification, although the orthogonality is exactly restored. Preferably equalization of the phase (SORC$_\gamma$) or even completely ignoring magnitude correction (EGC) results in much better performance. For SORC$_\gamma$ equalization, the choice of $\gamma = 0.4$ shows to be a good compromise between noise reduction and orthogonality for an OFDM-CDMA downlink transmission [11]. As can be seen, combining with MRC results in the lowest BER, although MRC does not address the orthogonality of the Walsh modulation, and, hence, yielding the highest self-interference of the Walsh symbols.

In order to illustrate the BER for M-ary Walsh modulation for different values of M, Fig. 4 presents a BER comparison for the values $M = 8$, 16 and $M = 32$. Furthermore, results for BPSK modulation are also plotted. MRC is applied for diversity combining; $J = 8$ active users and $N_2 = 64$ subcarriers are assumed.

The Walsh modulation shows a decreasing BER for larger values of M. This fact can mainly be explained by an increasing Euclidian distance (2). Additional system properties like less mismatching and less MAI (the number of subcarriers is increased, $N_M = 64 \cdot \log_2(M)$, see eq. (10)) further improve the performance. Furthermore, Walsh modulation performs better than BPSK modulation for $M \geq 16$ and an average $\bar{E}_b/N_0 > 4\,\mathrm{dB}$. For the same number of active users, note a gain of approximately $4.4\,\mathrm{dB}$ by an 32-ary Walsh modulation compared to BPSK

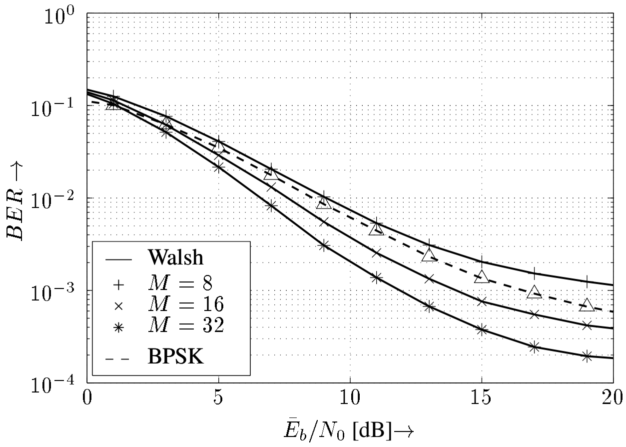

Figure 4: Comparison of $M = 8, 16, 32$-ary Walsh with BPSK modulation for $J = 8$ active users, $N_2 = 64$ subcarriers, and MRC

modulation at $BER = 10^{-3}$. Summarizing, the results express the improved signal constellation of the Walsh modulation as well as the profitable OFDM-CDMA properties for higher values M.

In previous discussions, less diversity of the Walsh chips has been achieved for the proposed system. Hence, if frequency-interleaving is applied, e.g. by a random frequency-interleaver in front of the OFDM-Modulation block, we will benefit from the frequency-selectivity of the channel which results in an additional improvement of the Walsh modulation. See section 5 for further results where aspects of channel coding are discussed, and frequency-interleaving is implemented.

4 Aspects of Decision-Directed Phase Estimation

A receiver, optimal in the ML sense, requires channel state information that has to be estimated. In this context, OFDM enables the exploitation of the channel in two dimensions, namely in time as well as in frequency direction, e.g. by pilot-aided channel estimation [10, 12]. A compound arrangement design of the training data in the time-frequency grid is necessary, and for interpolation it is possible to apply 1-D filtering, cascaded 1-D filters or 2-D filtering [10, 11]. Due to the necessary additional information, estimation based on training data results in less spectral efficiency.

In case of M-ary orthogonal modulation, the destruction of the orthogonality is mainly determined by phase rotation; each chip is multiplied by its own channel coefficient. Results in the previous section have shown that MRC is optimum in the ML sense, nevertheless, diversity combining with EGC where only the phase is corrected merely leads to moderate degradation (Fig. 3). Furthermore, with OFDM, channel state information is obtained by estimating only one single channel coefficient for each subcarrier. That implies the application of estimation techniques with low complexity. Due to the latter facts and to overcome the drawback of signaling overhead, we propose decision-directed phase estimation technique.

4.1 Decision Directed (DD) Receiver

With decision-directed (DD) phase estimation, the phase is estimated by comparison of the received signal with the decided symbols which are fed back under the assumption of correct decisions.
Fig. 5 illustrates the DD receiver for M-ary Walsh modulation. In contrast to the receiver shown in Fig. 2, the equalization block is expanded by the phase-estimation and an additional feedback with modulation and spreading of the decided group of $\log_2(M)$ bits (Fig. 1). Hence, (5) still holds where the equalization coefficient is given here by $E_i = \exp(-j\hat{\phi}_i)$, $i = 0, \dots, N_M - 1$, and $\hat{\phi}_i$ indicates the estimated phase for the i-th subcarrier (user $j = 0$ is assumed, and corresponding subscripts are omitted).

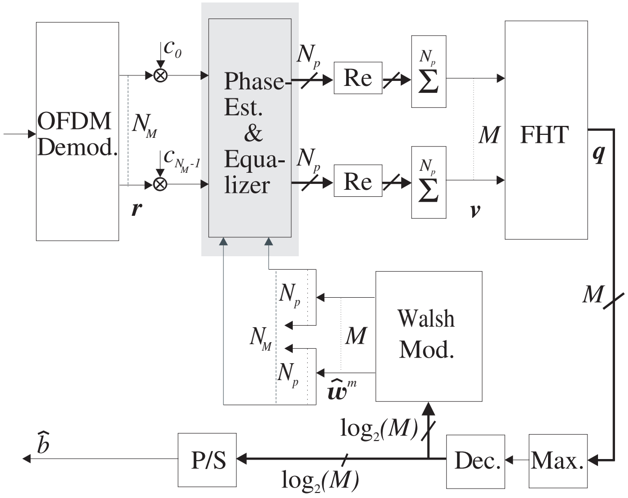

Figure 5: OFDM-CDMA receiver with DD phase estimation and MLD of Walsh symbols

In the following, we focus on the phase-estimation and equalization block. For simplicity, one of the subcarriers is considered (subscripts are omitted), and the different interference influences are modeled as AWGN. Such a subsystem for one subcarrier of this block is shown in Fig. 6. The

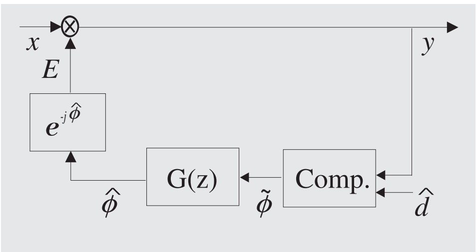

Figure 6: Phase-estimation and equalization subsystem

received signal x and the output signal y are given by

$$y = x \cdot E = |y| \cdot e^{j\Delta\phi}, \quad x = d \cdot H + n, \qquad (12)$$

where $d \in \{\pm 1\}$ represents the transmitted information symbol, $H = \rho \cdot \exp(\phi)$ the sub-channel coefficient, and n the AWGN with variance σ_n^2. The received signal is phase corrected by the multiplication with $E = \exp(-j\hat{\phi})$, and $\hat{\phi}$ denotes the estimated phase. The comparator performs the operation $\tilde{\phi} = \mathrm{Im}\left\{\hat{d} \cdot y\right\}$. According to the assumption of correct estimation ($\hat{d} = d$), the comparator output signal can be written as

$$\tilde{\phi} = \mathrm{Im}\left\{\hat{d} \cdot y\right\}\Big|_{\hat{d}=d} = \rho \cdot \sin(\Delta\phi) + \phi_n, \qquad (13)$$

with $\Delta\phi = \phi - \hat{\phi}$ as the phase of the output signal y and $\phi_n = \mathrm{Im}\{d \cdot E \cdot n\}$ as the phase noise. In case of proper phase tracking, $\Delta\phi$ is small and, hence, $\sin(\Delta\phi) \approx \Delta\phi$. We obtain the comparator output signal

$$\tilde{\phi} \approx \rho \cdot \Delta\phi + \phi_n. \qquad (14)$$

If statistical independence between data symbols and noise is assumed, the variance of the phase noise ϕ_n will be given by $\sigma_{\phi_n}^2 = 0.5\sigma_n^2$. Finally, the phase-correction is carried out after filtering $\tilde{\phi}$ by a first order loop (IIR-filter),

$$G(z) = a_0 \frac{z^{-1}}{1 - z^{-1}}, \qquad (15)$$

with gain parameter a_0. It is shown in [15] that the tracking performance and the noise interference of the system is mainly determined by a_0 (i.e. depending on the channel transmission conditions, the goal is to find a compromise between tracking performance and noise reduction ensuring system stability).

4.2 Comparisons of System Configurations

In this section, we investigate the proposed DD phase estimation by Monte-Carlo simulations and all given results refer again to the channel described in section 2.2. A gain parameter $a_0 = 1.5$ yields a good compromise between tracking performance, phase noise reduction, and system stability for the underlying indoor transmission conditions. It has to be pointed out that for DD reception steady state is considered; i.e. phase tracking is approached and no transposition of the first-order loop filter influences the system performance. Synchronization symbols, generally transmitted at the beginning of a transmission, can be used to pass the system into steady-state.
In all cases, $J = 8$ active users, $N_2 = 64$ subcarriers, and a velocity of $v_0 = 0.5$ m/s are assumed.

Fig. 7 shows the BER of DD estimation compared to EGC with perfectly known phases for 16-ary and 32-ary Walsh modulation (applying MRC requires the knowledge of the magnitudes and phases (6)). For approximately

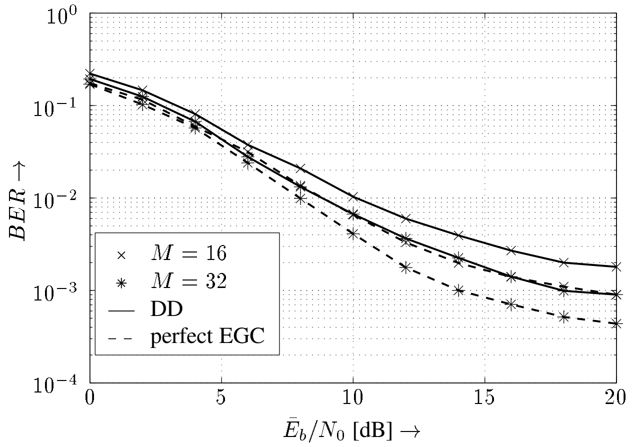

Figure 7: Comparison of DD phase estimation with perfect EGC for $M = 16, 32$-ary Walsh modulation, parameter $a_0 = 1.5$, $J = 8$ active users, and $N_2 = 64$ subcarriers

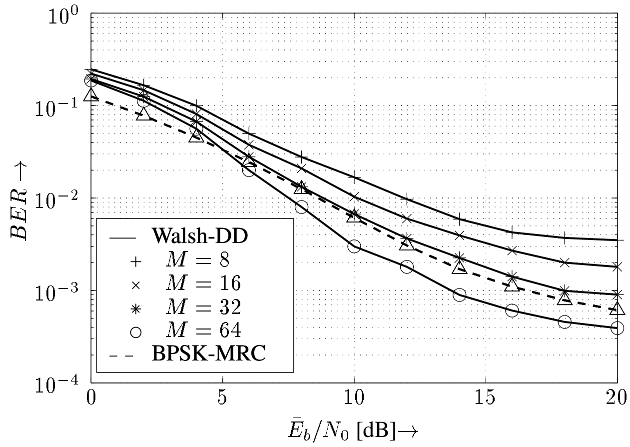

Figure 8: Comparison of M-ary Walsh modulation with DD reception ($a_0 = 1.5$) with perfect BPSK-MRC for $J = 8$ active users, $N_2 = 64$ subcarriers, and $v_0 = 0.5$ m/s

Table 2: Error-Floor: DD estimation compared with perfect EGC for $v_0 = 0.5$ m/s, $v_0 = 3.0$ m/s, and $M = 64$

v_0 in m/s	Error-Floor DD	Error-Floor perfect EGC
0.5	$\approx 4 \cdot 10^{-4}$	$\approx 2 \cdot 10^{-4}$
3.0	$\approx 2 \cdot 10^{-3}$	$\approx 2 \cdot 10^{-4}$

$\bar{E}_b/N_0 < 8$ dB, there is almost no loss in performance for the DD phase estimation. Due to the fact of MAI resulting in phase noise, there exists a moderate degradation for high ratios $\bar{E}_b/N_0$, i.e. the BER is not even doubled in these cases.

The error-floor performance with $M = 64$ and a higher velocity ($v_0 = 3.0$ m/s) is illustrated in Tab. 2. The gain parameters are again chosen to be a good compromise ($a_0 = 1.5$ for $v_0 = 0.5$ m/s and $a_0 = 19$ for $v_0 = 3$ m/s) ([3]). The results indicate the degradation in tracking performance of DD based estimations for higher velocities. With $v_0 = 0.5$ m/s, the error-floor of DD estimation is approximately 2 times higher than for perfect EGC compared to an approximately 10 times higher one for $v_0 = 3.0$ m/s.

For the remainder of the paper, $v_0 = 0.5$ m/s. In order to plainly show the principle performance of the DD based estimation for Walsh modulation, Fig. 8 reports, how the proposed system performs for different values of M. First of all, the results indicate that tracking is ensured independently of M, even for lower M-ary orthogonal modulation with more erroneous symbol decisions. Conceptually, the BER decreases for larger values of M turning out the properties like increasing Euclidian distance, reduced MAI, and less mismatching.

Fig. 8 also compares the Walsh modulation and DD reception with BPSK modulation, where BPSK modulation is combined with the more powerful equalization technique MRC [4, 12] (BPSK-MRC) with perfectly known channel coefficients. It should be emphasized that M-ary Walsh modulation with DD reception, and, therefore with nonperfect phase equalization, outperforms the BPSK-MRC scheme with the ideal assumption of perfectly known coefficients for values $M \geq 32$. The performance gain will be even higher if channel estimation is considered for BPSK modulation, e.g. pilot-symbol techniques. Furthermore, there is no redundancy required for the DD phase estimation which offers an additional coding gain in case of channel coding.

In the latter explanations of the DD reception, we proceed from a phase estimation block applied for each subcarrier. In order to reduce the complexity of the system, it is possible to benefit from non-frequency selective regions of the total bandwidth. This means, if the fading of adjacent subcarriers was statistically dependent, thus, the subcarriers were affected by the same phase deterioration, estimation could only be carried out once. For example, the channel described in section 2.2 has a coherence bandwidth of about 2.8 MHz. Since the available bandwidth equals 25 MHz, almost 11% of the used subcarriers is mutually statistically dependent ([4]). Consequently, complexity can be reduced tremendously.

5 Aspects of Channel Coding

In the previous sections, the Walsh modulation was introduced as an orthogonal modulation scheme. In addition to the interpretation as modulation concept, M-ary Walsh modulation can also be viewed as a *systematic linear block code* with code rate $\log_2(M)/M$. This interpretation opens

[3]Be aware of signal normalization with $1/N_M$ in each subcarrier after multiplication with the individual PN-code in the receiver. This fact influences the range of a_0 to ensure system stability.

[4]No frequency interleaving is assumed.

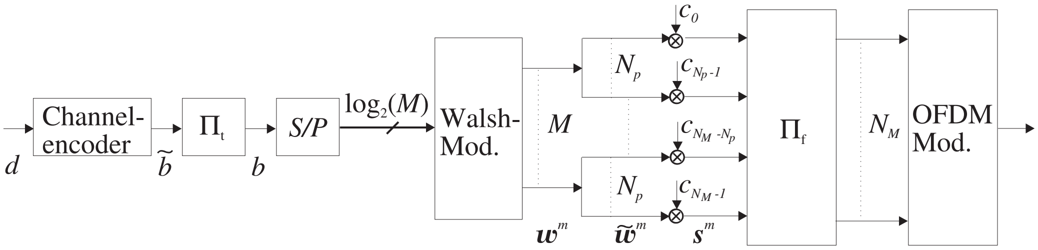

Figure 9: OFDM-CDMA transmitter with channel encoding and M-ary Walsh modulation

a completely new point of view especially with additional convolutional coding (CC) [20]. In this sense, combining CC and Walsh modulation represents a *serial concatenated coding scheme*: the CC as an outer code and the Walsh modulation as an inner block code. Hence, the system proposed is one possibility of low rate coding which is required in CDMA uplink systems with inherent high MAI. Other well-known schemes are, e.g., the QUALCOMM system (that is based on single carrier DS-CDMA and also uses M-ary Walsh modulation) or systems with one single powerful low rate channel code [13, 14, 23].
In contrast to these systems, the proposed one *(i)* incorporates a serial concatenation of codes, and *(ii)* it is embedded in OFDM-CDMA. Due to these differences, some important new aspects arise. First, decoding of Walsh symbols merely works in frequency direction, whereas the decoding of the outer CC is mainly arranged in time direction. Therefore, in case of mobile channels, the proposed coding scheme benefits from the selectivity of the channel in frequency as well as in time domain (e.g. large interleaver sizes can be avoided in case of low Doppler frequencies). Next, in order to carry out ML decoding of Walsh symbols, the Fast Hadamard Transform can be used. Hence, the Walsh modulation represents a *linear block code with low decoding complexity*.

In order to exploit the advantages of serial concatenated coding, soft decision, i.e. channel state information, has to be fed into the decoders [24]. Therefore, our first goal is to derive soft decision in the form of *bit specific reliability information* for the outer decoding scheme. Our derivations are based on [17, 25] with some specific modifications due to the application of OFDM-CDMA. Finally, we discuss the interchange between the rate of the CC R_c, the spreading of the Walsh modulation (changing M), and the simple replication (changing N_p), to approach high error-rate performance.

5.1 OFDM-CDMA TRANSMITTER WITH CC AND M-ARY ORTHOGONAL MODULATION

An OFDM-CDMA transmitter with channel encoding and Walsh modulation is illustrated in Fig. 9. One of J active users is shown, and corresponding subscripts are omitted.
The data bits $d \in \{0, 1\}$, each of duration T_d, are convolutionally encoded with code rate $R_c = K/N$. The input of the encoder is a sequence $\boldsymbol{d}$ of K subsequent data bits, and the output is the encoded bit sequence $\tilde{\boldsymbol{b}}$ of N bits, each with duration $T_b = R_c\, T_d$. After block interleaving (Π_t) in time direction, the encoded bits represent the data bits b at the input of the transmitter described in section 2.1 (Fig. 1). The transmitter explained in section 2.1 is additionally expanded by a frequency interleaver (Π_f) to achieve diversity for the Walsh chips, and, hence, to yield an additional diversity gain, even if no outer channel code ($R_c = 1$) is used. The interleaver scrambles vector $\boldsymbol{s}^m$ and passes it onto the OFDM modulator. Finally, OFDM modulation includes the IDFT and inserts the guard interval between adjacent OFDM symbols.

5.2 COHERENT OFDM-CDMA RECEIVER WITH SERIAL DECODING SCHEME

The receiver with serial decoding is shown in Fig. 10. The OFDM-CDMA receiver (first shadowed block) includes the OFDM demodulation, deinterleaving (Π_f^{-1}), multiplication with the user specific code, one tap equalization, real-part calculation, and correlation of N_p subcarriers, see 3.1, Fig. 2. Due to the results given in section 3.2.2,

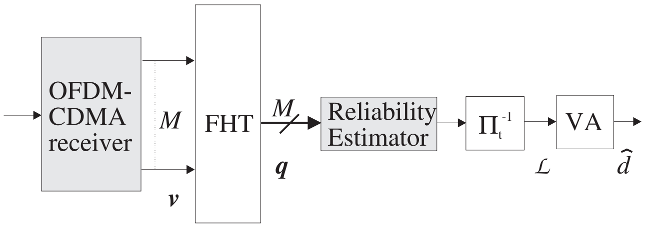

Figure 10: Ideal coherent OFDM-CDMA receiver with ML soft decoding of the outer code

the equalization scheme MRC (6) is implemented, and perfectly known channel coefficients are assumed. The FHT enables ML decoding of Walsh symbols, see section 3.1, and optimum decoding in the ML sense of the outer code is performed by the application of a soft input Viterbi algorithm (VA). Therefore, the reliability estimator uses the M decision variables to calculate the assigned bit specific log-likelihood ratio (LLR) $\mathcal{L}$ which is fed to the soft input Viterbi decoder after deinterleaving (Π_t^{-1}). Afterwards, we obtain the estimated data stream with bits $\hat{d}$.

For CDMA systems, the BER can be reduced by an optimized compound design of channel coding and spreading. Here, the product between bandwidth and bit duration is given by

$$B\,T_d = \underbrace{\frac{M}{\log_2(M)} \cdot \frac{N_p}{R_c}}_{P_G} \cdot \frac{T}{T-T_g}. \qquad (16)$$

The first term of (16) describes the spreading of the Walsh modulation, the second one the ratio of simple spreading (N_p) over the code rate R_c of the channel code, whereas the third term takes into account the guard time T_g. For our comparisons, the product $B\,T_d$ remains unchanged due to the exploitation of the inherently overall spreading factor ([5]) P_G. In order to analyze the trade-off between spreading and coding, the data rate $R = 1/T_d$ is based on binary modulation without channel coding ($R_c = 1$), and the bandwidth B is generally given.

5.3 Evaluation of Bit-Specific Soft Values

In the following, we will derive the bit specific log-likelihood criterion for ML soft decision decoding of the outer CC in case of Walsh modulation applied as inner block code. The MAI is taken into account as AWGN, and independent adjacent fading subcarriers ensured by perfect frequency interleaving (Π_f) are assumed.

5.3.1 *Antipodal Transmission*

Let us first consider binary antipodal transmission on a single carrier system with $b_\kappa \in \{-1,+1\}$ denoting the κ-th transmitted encoded bit. Hard decision at the receiver leads to the binary encoded bit $z_\kappa \in \{-1,+1\}$. For a memoryless discrete binary symmetric channel the likelihood criterion for ML soft decision channel decoding is given by [26]

$$\Phi_{ML}^{BSC} = \sum_\kappa b_\kappa \underbrace{z_\kappa \ln \frac{P_\kappa}{1-P_\kappa}}_{\triangleq\ \mathcal{L}_\kappa} \stackrel{!}{=} \max\,, \qquad (17)$$

where $P_\kappa \triangleq P(z_\kappa = b_\kappa)$ denotes the probability for correct decision. The likelihood criterion can efficiently be solved by the VA where the LLR $\mathcal{L}_\kappa = z_\kappa L_\kappa$ serves as a soft input signal. In this context, the absolute value $L_\kappa = \ln \frac{P_\kappa}{1-P_\kappa}$ of the LLR can be interpreted as a reliability indicator for the hard decided code bit z_κ. Due to the fact that $\mathcal{L}_\kappa$ involves channel state information, the application of (17) results in optimum performance under time-variant channels. For example, if the transmitted signal b_κ suffers from fading h_κ and is disturbed by AWGN, the LLR can be expressed as

$$\mathcal{L}_\kappa = h_\kappa \frac{4E_s}{N_0} r_\kappa, \qquad (18)$$

where r_κ denotes the received signal after matched-filtering, E_s is the symbol energy and $N_0/2$ indicates the Gaussian noise spectral density [26].
In case of OFDM-CDMA with antipodal transmission, the derivation of the LLR yields an equivalent expression as (18), and several approaches are given for a downlink transmission in [12]. Derivations for the uplink result in approximately the same approaches except of individual channel transfer functions for each specific user.

5.3.2 *M-ary Orthogonal Modulation*

Let us now return to the problem of M-ary orthogonal modulation with MRC detection. Here, it is also possible to describe the reliability estimator based on hard symbol decision. Fig. 11 shows the corresponding reliability estimator model.

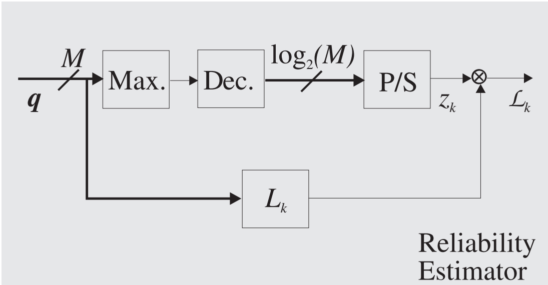

Figure 11: Reliability estimator model

The choice of the maximum value of vector $\boldsymbol{q}$ results in symbol decision. Decoding of the decided symbol to $\log_2(M)$ data bits and parallel/serial conversion leads to the estimated bits z_κ. Subsequently, the hard decided bits are multiplied with the reliability indicator L_κ to form the bit specific soft input signal $\mathcal{L}_\kappa$ for the VA.
In order to derive the bit specific reliability estimator $\mathcal{L}_\kappa$, we proceed from the derivation given in [17, 25], where non-coherent reception in a DS-CDMA system is considered. We start with the calculation of the (symbol) a-posteriori probability (APP) that $\boldsymbol{\omega}^n$ is the transmitted symbol under observation of $\boldsymbol{q}$. Furthermore, one time instant and user $j = 0$ are taken into account (subscripts are omitted). Applying Baye's law results in

$$P(\boldsymbol{\omega}^n|\boldsymbol{q}) \;=\; \frac{P(\boldsymbol{\omega}^n)}{p(\boldsymbol{q})} \cdot p(\boldsymbol{q}|\boldsymbol{\omega}^n)\,. \qquad (19)$$

If equiprobable transmitted symbols $\boldsymbol{\omega}^n$ are assumed, we obtain $P(\boldsymbol{\omega}^n) = 1/M$. Due to the statistical independence of the components of $\boldsymbol{q}$, the conditional probability density function $p(\boldsymbol{q}|\boldsymbol{\omega}^n)$ can be written as the product

$$p(\boldsymbol{q}|\boldsymbol{\omega}^n) = r(q_0) \cdot \ldots \cdot R(q_n) \cdot \ldots \cdot r(q_{M-1}), \qquad (20)$$

with distributions $r(q_m) = p(q_m|\boldsymbol{\omega}^n)$ for $m \neq n$, and $R(q_n) = p(q_n|\boldsymbol{\omega}^n)$. The terms $r(q_m)$ and $R(q_n)$ can be calculated uniquely. In case of the considered coherent

[5] Being aware of a changed symbol duration T.

MRC detection, we obtain a zero mean Gaussian distribution with variance σ_q^2 for the m-th component, where the hypothesis $\boldsymbol{\omega}^n$ does not hold ([6]):

$$r(q_m) = \frac{1}{\sqrt{2\pi\sigma_q^2}} \exp\left(-\frac{q_m^2}{2\sigma_q^2}\right), \quad \forall\, m \neq n. \tag{21}$$

On the other hand, for the n-th component corresponding to the current hypothesis $\boldsymbol{\omega}^n$, the FHT results in a Gaussian distribution

$$R(q_n) = \frac{1}{\sqrt{2\pi\sigma_q^2}} \exp\left(-\frac{(q_n - E_H)^2}{2\sigma_q^2}\right) \tag{22}$$

with mean $E_H = E\left\{\frac{1}{N_M}\sum\limits_{i=0}^{N_M-1}|H_i|^2\right\}$, where $E\{\cdot\}$ denotes the expected value, and H_i describes the channel coefficient.
With (21), (22), and additionally defining the probability density function

$$r(q_n) \triangleq \frac{1}{\sqrt{2\pi\sigma_q^2}} \exp\left(-\frac{q_n^2}{2\sigma_q^2}\right), \tag{23}$$

we can rewrite (19) in the form

$$P(\boldsymbol{\omega}^n|\boldsymbol{q}) = \underbrace{\frac{1/M}{p(\boldsymbol{q})} \prod_{m=0}^{M-1} r(q_m)}_{\triangleq\, \rho} \cdot \frac{R(q_n)}{r(q_n)}, \tag{24}$$

with $n \in \{0, \ldots, M-1\}$.The unknown factor ρ can be determined indirectly by the exploitation of the relationship

$$\sum_{n=0}^{M-1} P(\boldsymbol{\omega}^n|\boldsymbol{q}) = \rho \cdot \sum_{n=0}^{M-1} \frac{R(q_n)}{r(q_n)} = 1 \tag{25}$$

(the union of all elementary events has probability one). With (22) and (23), the calculation of

$$\frac{R(q_n)}{r(q_n)} = \exp\left(\frac{2\, q_n\, E_H - E_H^2}{2\sigma_q^2}\right) \tag{26}$$

requires the knowledge of the noise variance σ_q^2 and the expected value of the average channel energy over all subcarriers E_H.

These parameters can be estimated as follows:
(*i*) *noise variance estimation*
Assuming that the decision variable with maximum magnitude, denoted by q_l, represents the true hypothesis, we evidently obtain an estimate of the noise power $\hat{\sigma}_q^2$ by the mean over $M-1$ components $q_m, m \neq l$, containing the false hypotheses:

$$\hat{\sigma}_q^2 = \frac{1}{M-1} \cdot \sum_{\substack{m=0 \\ m\neq l}}^{M-1} q_m^2\,. \tag{27}$$

[6]In contrast to the non-coherent DS-CDMA system with chi-square distribution [25].

(*ii*) *average channel energy estimation*
If we assume statistically independent fading subcarriers and the same average energy on all subcarriers, we can estimate E_H by the mean over all subcarriers:

$$\hat{E}_H = \frac{1}{N_M} \sum_{i=0}^{N_M-1} |H_i|^2. \tag{28}$$

With (25)-(28), all parameters required for calculation of the symbol APP (24) are known. The results can be summarized for all M hypotheses: If the symbols $\boldsymbol{\omega}^n$ are replaced by their corresponding bit patterns $\{b_0, \ldots, b_{\log_2(M)-1}\}$ in antipodal representation, we can express the symbol APP's in the form (e.g. for $M = 16$)

$$\begin{aligned} P(-1,-1,-1,-1|\boldsymbol{q}) &= \rho \cdot R(q_0)/r(q_0) \\ P(-1,-1,-1,+1|\boldsymbol{q}) &= \rho \cdot R(q_1)/r(q_1) \\ &\vdots \\ P(+1,+1,+1,+1|\boldsymbol{q}) &= \rho \cdot R(q_{M-1})/r(q_{M-1}). \end{aligned} \tag{29}$$

The application of (17) requires knowledge of the probabilities of individual bit decisions which can be gained by a column-wise derivation of (29). Note, at first, that (17) does not depend on the specific choice of the decision for bit z_κ, since

$$z_\kappa = +1 \;\rightarrow\; z_\kappa \cdot L_\kappa \quad = +\ln \frac{P(b_\kappa = +1|\boldsymbol{q})}{1 - P(b_\kappa = +1|\boldsymbol{q})}$$

and

$$\begin{aligned} z_\kappa = -1 \;\rightarrow\; z_\kappa \cdot L_\kappa \quad &= -\ln \frac{P(b_\kappa = -1|\boldsymbol{q})}{1 - P(b_\kappa = -1|\boldsymbol{q})} \\ &= +\ln \frac{P(b_\kappa = +1|\boldsymbol{q})}{1 - P(b_\kappa = +1|\boldsymbol{q})} \end{aligned}$$

yield the same expression.
Now, consider the calculation of soft information, e.g. for the first bit b_0 of the $\log_2(M)$-bit groups (most left bit-"column" in (29)): Adding all probabilities belonging to '$b_0 = +1$' results in

$$P(b_0 = +1|\boldsymbol{q}) = \sum_{n=M/2}^{M-1} P(\boldsymbol{\omega}^n|\boldsymbol{q}). \tag{30}$$

This leads to the reliability information for the first bit of the Walsh symbol being '$b_0 = +1$'

$$\mathcal{L}_0 = \ln \frac{P(b_0 = +1|\boldsymbol{q})}{1 - P(b_0 = +1|\boldsymbol{q})} \tag{31}$$

and serves as a soft input for the Viterbi channel decoder. The other bits $b_1, \ldots, b_{\log_2(M)-1}$ are treated equivalently.

5.4 Comparisons of System Configurations

Again, the following results are given for a transmission over an indoor Rayleigh fading channel related to the

European HIPERLAN/2 standardization and described in detail in section 2.2. Due to the very low Doppler frequency of $f_{d,max} = 9\,\mathrm{Hz}$, the fading on each subcarrier is highly statistically dependent. Since the serial decoding scheme operates in frequency (inner Walsh modulation) as well as in time (outer CC) direction, burst error structures can be avoided by sufficient frequency interleaving.
First, the indoor channel is modeled assuming sufficient frequency interleaving. Subsequently, we take into account an exponential delay profile with a maximum delay of $\tau_{max} \approx 350\,\mathrm{ns}$, and a coherence bandwidth of about 2.8 MHz, see section 2.2. I.e. the number of *independent* subcarriers is reduced dramatically.
The trade-off between coding and spreading is carried out for an unchanged product $B\,T_d$ (16) and is based on binary modulation without CC with $N_2 = 64$ subcarriers. The guard time is chosen to be $T_g = 640\,\mathrm{ns}$ due to the system design based on binary modulation with $T_g/T = 0.2$, see section 3.2.1. This system design results in a data rate of $R = 312.5$ kbit/s for all cases of spreading and coding. A block interleaver (Π_t) with 32 rows and 18 columns is used to separate the channel code and the M-ary Walsh modulation. We employed two convolutional codes of rate $R_c = 1/2$ and $R_c = 1/3$, both with constraint length 7 [15]. For all cases, $J = 8$ active users are taken into account, and perfect channel estimation as well as perfect synchronization are assumed for the user concerned.

Fig. 12 shows the BER of the M-ary Walsh modulation for $M = 16$ and $M = 32$ by sharing P_G between simple spreading N_p and convolutional coding of rate R_c (16). Independent of the M-ary modulation, the results indicate that choosing a higher amount of simple spreading N_p combined with less powerful CC ($R_c = 1/2$) outperforms the scheme with lower amount N_p combined with more powerful CC ($R_c = 1/3$). Note the gain of about 1 dB in $\bar{E}_b/N_0$ at a BER of 10^{-3} for the 32-ary modulation. This fact can be explained for $R_c = 1/3$ by a higher loss of $\bar{E}_b/N_0$ due to an unchanged guard time T_g, but a shorter symbol duration T, and an additional lower energy of the coded bit in front of the Viterbi decoder ([7]) . Moreover, a lower number of subcarriers ($N_M = M \cdot N_p$) results in higher MAI in case of the used PN-codes. Hence, the more powerful CC is not able to compensate for the summarized losses [27].

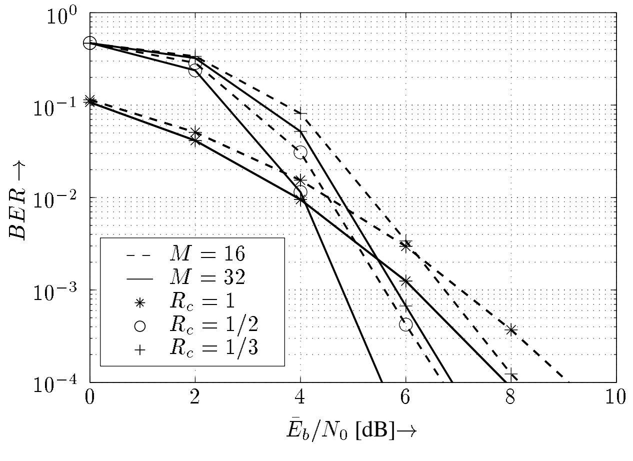

Figure 12: Sufficient frequency interleaving: Trade-off between CC, M-ary Walsh modulation, and simple spreading for $M = 16,\ 32$, and code rates $R_c = 1,\ 1/2,\ 1/3$

We now focus on the trade-off between M-ary Walsh modulation and CC (N_p remains unchanged due to an unchanged $B\,T_d$ (16)). For example, 32-ary modulated signals with code of rate $R_c = 1/2$ yield a gain of $\bar{E}_b/N_0 \approx 2$ dB in comparison with 16-ary Walsh modulation with $R_c = 1/3$ at BER=10^{-3}. This results from an increasing Euclidian distance (2) for higher values M and less MAI (higher number of subcarriers). In fact, the quality of the FHT output is decisive for the overall system performance.

The simulation results in Fig. 13 show the BER for the transmission over an indoor channel with coherence bandwidth of about 2.8 MHz. BPSK modulation and 32-ary Walsh modulation are considered. In contrast to Fig. 12, Fig. 13 indicates a significant loss of the Walsh modulation due to the statistical dependence of the adjacent subcarriers. This degradation is mainly caused by insufficient frequency interleaving. There exists only a slight degradation because of assuming independent subcarriers for the derivations of the log-likelihood ratios. Most important, Fig. 13 expresses that BPSK modulation even combined with convolutional coding leads to an unacceptable BER for an OFDM-CDMA uplink transmission over an indoor Rayleigh fading channel ([8]). Moderate performance will only be achieved if M-ary Walsh modulation is applied.

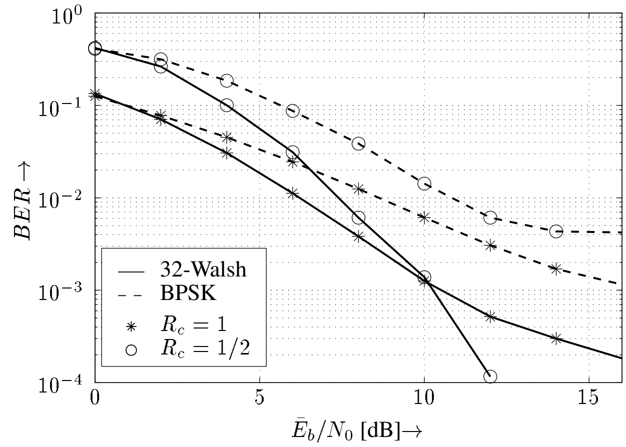

Figure 13: Insufficient frequency interleaving: Comparison of 32-ary Walsh modulation with BPSK, $R_c = 1,\ 1/2$

[7] $\bar{E}_b$ denotes the bit energy at the output of the Viterbi decoder.
[8] Results which are not shown in Fig. 13 indicate that the BER will further increase, if CC with a lower rate than $R_c = 1/2$ is used.

6 CONCLUSION

In this paper, we have proposed the application of M-ary Walsh modulation as an optimized inner spreading for an OFDM-CDMA uplink indoor transmission. Examination of general system properties like mismatching and MAI confirm the optimization; note the gain of about 0.8 dB in SNR by raising M form 2 to 32 due to less mismatching. Moreover, M-ary Walsh modulation reveals to outperform BPSK modulation already for $M \geq 16$.

Decision-directed phase estimation has been suggested for channel phase estimation leading to moderate performance loss in comparison with perfect phase equalization. It should be emphasized that M-ary Walsh modulation with decision-directed phase estimation (i.e. non-perfect phase equalization) outperforms the BPSK-MRC scheme (BPSK with ML-optimum equalization assuming perfect magnitude and phase estimation) for values $M \geq 32$.

In the context with channel coding, the proposed system represents a serial concatenated coding scheme. It operates in time as well as frequency domain, and thus, it exploits diversity in both domains. Furthermore, the FHT enables ML decoding of Walsh symbols with low complexity. In order to perform ML soft decoding of the outer convolutional code, a derivation of bit specific soft information has been given. Analysis concerning the trade-off between coding and spreading shows to better lay stress on the inner system with a less powerful outer channel code. Again, the proposed concatenated coding scheme indicate the significant optimization compared with BPSK modulation and convolutional coding. BPSK modulation even combined with powerful convolutional coding leads to an unacceptable BER.

Summarizing, M-ary Walsh modulation reveals to be an elaborate modulation scheme suitable for OFDM-CDMA. New aspects will arise by iterative decoding being a main objective in future work. Finally, the extension of multi-user-detection methods is quit obvious.

Acknowledgement

The authors would like to express their thanks to the anonymus reviewers for their helpful comments and suggestions.

Manuscript received on . . .

REFERENCES

[1] K. Fazel and L. Papke. On the performance of convolutionally-coded CDMA/OFDM for mobile radio communication systems. In *Proc. IEEE Int. Symp. on Personal, Indoor and Mobile Radio Communications (PIMRC)*, pages D3.2.1–D3.2.5, September 1993.

[2] N. Yee, J.-P. Linnartz, and G. Fettweis. Multi-Carrier CDMA in Indoor Wireless Radio Networks. In *Proc. IEEE Int. Symp. on Personal, Indoor and Mobile Radio Communications (PIMRC)*, pages D1.3.1–D1.3.5, September 1993.

[3] L. Vandendorpe. Multitone Spread Spectrum Multiple-Access Communications System in a Multipath Rician Fading Channel. *IEEE Trans. on Vehicular Technology*, Vol. 44, No. 2, pages 327–337, May 1995.

[4] R. Prasad. *CDMA for Wireless Personal Communication.* Artech House, Norwood, 1996.

[5] S. Hara and R. Prasad. Overview of Multicarrier CDMA. *IEEE Communications Magazine*, Vol. 35, No. 12, pages 126–133, December 1997.

[6] G. Fettweis, K. Anvari, and A. Shaikh Bahai. On Multi-Carrier Code Division Multiple Access (MC-CDMA) Modem Design. In *Proc. IEEE Vehicular Technology Conference (VTC)*, pages 1670–1674, June 7–11 1994.

[7] S. Kaiser. On the Performance of Different Detection Techniques for OFDM-CDMA in Fading Channels. In *Proc. IEEE Global Conference on Communications (GLOBECOMM)*, pages 2059–2063, November 13–17 1995.

[8] J. Egle, M. Reinhardt, and J. Lindner. Equalization and Coding for Extended MC-CDMA Over Time and Frequency Selective Channels. In G.P. Fettweis and K. Fazel, *Multi-Carrier Spread-Spectrum*, pages 127–134. Kluwer Academic, The Netherlands, 1997.

[9] N. Yee and J.-P. Linnartz. Wiener Filtering of Multi-Carrier CDMA in a Rayleigh Fading Channel. In *IEEE/ICCC Conference on Personal Indoor Mobile Radio Communications and Wireless Computer Networks (WCN)*, pages 1344–1347, Sept. 1994.

[10] P. Hoeher, S. Kaiser, and P. Robertson. Pilot-Symbol-Aided Channel Estimation in Time and Frequency. In *Proc. International Conference on Acoustics, Speech and Signal Processing (ICASSP)*, pages 1845–1848, April 21-24 1997.

[11] T. Mueller, K. Brueninghaus, and H. Rohling. Performance of coherent OFDM-CDMA for Broadband Mobile Communications. *Wireless Personal Communications*, No. 2, pages 295–305, 1996.

[12] Stefan Kaiser. *Multi-Carrier CDMA Mobile Radio Systems – Analysis and Optimization of Detection, Decoding and Channel Estimation*. PhD thesis, German Aerospace Center, VDI, January 1998.

[13] R.A. Stirling-Gallacher and G.J.R. Povey. Different Channel Coding Strategies for OFDM-CDMA. In *Proc. IEEE Vehicular Technology Conference (VTC)*, pages 845–849, May 4-7 1997.

[14] J. J. Maxey and R. F. Ormondroyd. Multi-Carrier CDMA using Convolutional Coding and Interference Cancellation over Fading Channels. In G.P. Fettweis and K. Fazel, *Multi-Carrier Spread-Spectrum*, pages 89–96. Kluwer Academic, The Netherlands, 1997.

[15] J.G. Proakis. *Digital Communications*. McGraw–Hill, 3-rd edition, 1995.

[16] A.J. Viterbi. *CDMA – Principles of Spread Spectrum Communication*. Addison–Wesley, 1995.

[17] M. Benthin, K.D. Kammeyer, R. Mann Pelz, and D. Nikolai. On the Optimisation of a Noncoherent CDMA System Based on *M*-ary Orthogonal Modulation. *European Trans. on Telecommunications*, Vol. 9, No. 6, pages 497–506, November 1998.

[18] A. Dekorsy and K.D. Kammeyer. M-ary Orthogonal Modulation for MC-CDMA Systems in Indoor Wireless Radio Networks. In G.P. Fettweis and K. Fazel, *Multi-Carrier Spread-Spectrum*, pages 69–76. Kluwer Academic, The Netherlands, 1997.

[19] A. Dekorsy and K.D. Kammeyer. M-ary Orthogonal Modulation for Multi-Carrier Spread-Spectrum Uplink Transmission. In *Proc. IEEE International Conference on Communications (ICC)*, pages 1004–1008, June 7–11, 1998.

[20] A. Dekorsy, S. Fischer, and K.D. Kammeyer. Maximum Likelihood Decoding of M-ary Orthogonal Modulated Signals for Multi-Carrier Spread-Spectrum Systems. In *Proc. IEEE Int. Symp. on Personal, Indoor and Mobile Radio Communications (PIMRC)*, September 1998.

[21] P. A. Bello. Characterization of randomly time-invariant linear channels. *IEEE Trans. on Comm. Syst.*, pages 360–393, December 1963.

[22] K.D. Kammeyer. *Nachrichten"ubertragung*. B.G. Teubner, Stuttgart, 2-nd edition, 1996.

[23] A.J. Viterbi. Very Low Rate Convolutional Codes for Maximum Theoretical Performance of Spread–Spectrum Multiple–Access Channels. *IEEE Journal on Selected Areas in Comms*, Vol. 8, No. 4, pages 641–649, May 1990.

[24] J. Hagenauer. Soft–In / Soft–Out: The Benefits of Using Soft Values in all Stages of Digital Receivers. In *Proc. 3rd Int. Workshop on DSP Techniques Applied to Space Comm.*, September 1992.

[25] M. Benthin and K.D. Kammeyer. Viterbi Decoding of Convolutional Codes with Reliability Information for a Noncoherent RAKE-Receiver in a CDMA-Environment. In *Proc. IEEE Global Conference on Communications (GLOBECOMM)*, pages 1758–1762, November/December 1994.

[26] J. Hagenauer. Viterbi Decoding of Convolutional Codes for Fading- and Burst–Channels. In *Proc. of the 1980 Zurich Seminar on Digital Communications*, pages G2.1–G2.7, 1980.

[27] D. Nikolai, K.D. Kammeyer, and A. Dekorsy. On the Bit Error Behaviour of Coded DS-CDMA with Various Modulation Techniques. In *Proc. IEEE Int. Symp. on Personal, Indoor and Mobile Radio Communications (PIMRC)*, September 1998.